HYDROLOGICAL PROCESSES
*Hydrol. Process.* **21**, 1115–1124 (2007)
Published online 12 December 2006 in Wiley InterScience
(www.interscience.wiley.com) DOI: 10.1002/hyp.6301

# A validated fast algorithm for simulation of flooding events in plains

D. Dalponte,[1] P. Rinaldi,[1] G. Cazenave,[2] E. Usunoff,[2] L. Vives,[2] M. Varni,[2] M. Vénere[3] and A. Clausse[3]*

[1] *PLADEMA-ISISTAN-CICPBA, Universidad Nacional del Centro, 7000 Tandil, Argentina*
[2] *IHLLA-CICPBA, Universidad Nacional del Centro, 7300 Azul, Argentina*
[3] *CNEA-CONICET, Universidad Nacional del Centro, 7000 Tandil, Argentina*

## Abstract:

Hydrological modelling in large plains is not a straightforward task owing to the crucial influence of several elements, namely, accumulation of water on local depressions, absence of an integrated drainage network, generalized meagre surface slopes, strong sensitivity of the soil water content before rainfall events, and variation of the soil infiltration capacity with numerous transient and local factors. It would then appear that distributed hydrological models (DHM) are prone to produce better results than lumped-parameter models. The trade-off in setting up a DHM, however, is how realistic its results are as compared to its simplicity.

This paper presents a physically based DHM, named AQUA, which can handle large domains discretized in squared cells of typically 80 m a side. In order to address properly the flow resistance, it relies on a relaxation parameter ($\alpha$) with different values for the watercourses and the terrain. Likewise, an infiltration function ($I$) regulates the downward movement of water. Moreover, the model is supported by an adequate description of the gentle topographical features, which was achieved by a digital elevation model (DEM) from radar interferometry.

The testing phase took into account the Santa Catalina Creek Basin (158 km$^2$, centre Buenos Aires Province in Argentina). The results were quite encouraging, as the model was able to reproduce the effect of various rainfall scenarios. Sensitivity analyses of the model parameters were consistent with the actual simulation results. AQUA was tested against the well-known HEC-1 model, with a fairly good match of their results. Copyright © 2006 John Wiley & Sons, Ltd.

KEY WORDS distributed hydrological models; large plains flooding; cellular automata

*Received 14 September 2005; Accepted 20 March 2006*

## INTRODUCTION

Simulations of surface flow in landscape models play an important driving role in floodplain management. Surface water flow is a major transport mechanism in plain hydrology, either by delivering the elements to the biota or by removing the constituents in excess. Although considerable efforts have been put in creating adequate models for various landscapes, still there is no universal code that can be easily adapted for a wide range of applications. Substantial efforts are needed to tune the existing models to the specifics on each landscape and the goals of the study.

In general, hydrologic models are part of more complicated modelling structures, therefore requiring simple algorithms to run within the framework of the entire ecological scenario. Consequently, some details should be sacrificed in order to make the numerical calculation feasible. An important trade-off in hydrologic models is the coarser spatial and temporal resolution that should be employed (kilometers and days), in contrast to small scale flows (meters and seconds). The classical numerical methods, as finite differences or finite elements, can hardly be afforded in the former case.

Previous numerical modelling of floodplain hydrology has ignored fluxes of water to and from the surrounding hill slopes. However, the current understanding of floodplain hydrology suggests that hill slope water levels play an important role in fluxes into and out of the alluvium. At present, we still do not know what process representation should be included in a floodplain inundation model to achieve given levels of predictive ability. Ultimately, the best model will be the simplest one that provides relevant information while reasonably fitting the available data.

The kinetic wave approximation of the St Venant equations is a popular tool that has been applied to the simulation of linear flood routing in rivers. On the other hand, in dealing with two-dimensional overland flows, explicit numerical schemes were used (Abbott *et al.*, 1986). Explicit methods are appropriate when complex boundaries cannot be avoided, but they are stability dependent on the spatial and temporal resolution. Thus, a clear scope exists for a combined modelling and field monitoring of hydrological interactions within lowland floodplains while maintaining the simplicity necessary for feasible computations.

* Correspondence to: A. Clausse, Universidad Nacional del Centro, 7000 Tandil, Argentina. E-mail: clausse@exa.unicen.edu.ar

Flows in rivers and floodplains are usually characterized by means of local spatial fields representing the fluid velocity and the surface water height (stage). In such representations, surface flows are described with partial differential equations in terms of the fields representing the physical variables. Freeze and Harlan, 1969. proposed physically based models, discretizing the basins and describing the spatial and temporal behaviour of the hydrological processes by means of partial differential equations that are solved by numerical methods. The SHE model (Abbott *et al*., 1986) is a well-known model produced according to those premises. Generally, the application of models according to that philosophy is restricted to small basins.

In the 1950s, Ulam and von Neumann (Cooper, 1987) conceived the idea of an ingenious mathematical tool called cellular automata (CA). They realized that certain complex phenomena might be simulated as assemblies of finite cells, which interact according to a small number of simple rules based on heuristic considerations. The interaction rules, generally applied to the immediate neighbours, may or may not bear a resemblance to the actual physical laws governing the phenomena at hand. However, for fluids, it was found that the statistical averages tend to the solution of the partial differential equations known to govern the situation—typically, the Navier-Stokes equation (Wolfram, 1986). More recently, numerical simulations of sand piles have shown that complex systems amenable to representation by cellular automata exhibit certain regularities in their global behaviour, thus raising hope that quantitative laws might be formulated to encompass disparate phenomena: earthquakes, stock markets, weather, biological systems, etc.

In this article, a novel perspective in the modelling of surface flows in large plains, based on virtual landscapes created using cellular automata, is presented. The model is able to provide the evolution of the flow variables by tracking local water stocks, bookkeeping precipitation, infiltration, evapotranspiration, and intercell flows. Thus, while retaining the basic philosophy underlying cellular automata, a realistic model of surface flows is obtained, offering a useful tool for the modelling of floodings in plains.

## THE AQUA AUTOMATA

Hydrological processes in extensive plains differ considerably from those characterizing hilly and mountainous areas (sloping terrains, in general). Though the structure of the hydrological cycle and the water balance equations are not modified by the morphological, geological and pedological conditions, the weighting of the various components does change, i.e. the vertical flows prevail over the horizontal ones. The main feature of plains is that their surface has no slope or the slopes are negligible. Local depressions cover the terrain instead of well-developed natural drainage systems (integrated river network), because the morphological energy-content of the system characterized by the difference in height between the highest point of the basin and the outflow section is extremely low.

The precipitations are stored in terrain depressions, forming shallow ponds and marshes. On sloping terrain this storage is generally negligible, but the amount of water accumulated in the local depressions of flat areas might substantially exceed the other terms of the water balance equation. A considerable part of this water evaporates and infiltrates (Varni *et al*., 1999). Surface runoff from the neighbouring hilly areas increases the amount of water covering the plain: even the watercourses coming from higher areas may vanish in the plain and the water carried by them run over the surface—several rivers of Argentine Pampas often follow that behaviour. The water exceeding the storage capacity of the depressions moves on the surface very slowly as sheet flow. Infiltration and evaporation is generally high because of the long duration of the pounded water. Given the negligible slope of the terrain, an important consequence can be drawn up from this fact: human activities modify the equilibrium of the plains; thus, any model has to be able to incorporate those actions (roads, channels mainly).

The first requirement for a better understanding of the plains surface hydrology is a detailed analysis of the storage processes in depressions, in the soil and groundwater zones. Therefore, any model that simulates the dominant processes in the surface water in plains should:

1. Be spatially distributed, for the lineal fluxes are not well defined.
2. Incorporate a good spatial description of the terrain depressions, which in turn requires accurate digital elevation models (DEMs) with fine grid sizes.

Following the mentioned criteria, let us describe the physical terrain by means of a DEM, consisting of a scalar field, $h\ (x, y)$, associated to a two-dimensional grid. The field $h\ (x, y)$ represents the average vertical coordinate of each spatial cell. Following the CA paradigm, the surface state of each cell is determined by a scalar $w\ (x, y)$, representing in our case the water level in the cell $(x, y)$.

Now let us imagine the cells connected by floodgates that are opened and closed in turns, allowing the water to flow driven by the elevation differences between cells. Additionally, water mass sources and sinks can be associated to each cell, accounting for infiltration, precipitation, and inflows and outflows due to seepage or evapotranspiration.

### *Water distribution rule*

The surface flow is simulated by applying a basic water distribution rule on isolated partitions of the spatial domain. The basic partition is a set of $3 \times 3$ cells (Figure 1). By means of the rule, the water is distributed



DOI: 10.1002/hyp

Figure 1. Basic partition

inside each basic partition according to the following procedure:

1. Order the cells index according to the terrain height, that is:

$$h_1 \leq h_2 \leq \ldots \leq h_9 \tag{1}$$

2. Let $w_i^{old}$ be the current water level of the $i$-cell.
3. Calculate the equilibrium surface water height, $H$, as the height the water would reach, provided that the total water volume contained in the partition drains down to the lowest possible locations (Figure 2), that is:

$$H = \frac{W + \sum_{i=1}^{k} h_i}{k} \tag{2}$$

where $W$ is the water volume contained in the partition divided by the unit-cell area that can be calculated as:

$$W = \sum_{i=1}^{9} (w_i^{old} - h_i) \tag{3}$$

Figure 2. Equilibrium state when the water is drained down in a basic partition

and $k$ is the number of cells that remains wet after the water drains down, which is the largest cell index satisfying:

$$W \geq \sum_{i=1}^{k} (h_k - h_i) \tag{4}$$

4. Calculate the drained water level, $w_i^{drain}$, that would have the cells if the water volume contained in the partition drains down to the lowest locations (Figure 2), that is:

$$\begin{aligned} w_i^{drain} &= H - h_i \quad if \quad i \leq k \\ w_i^{drain} &= 0 \quad if \quad i > k \end{aligned} \tag{5}$$

5. Calculate the new water level of the cells as a linear combination of $w_i^{old}$, and $w_i^{drain}$:

$$w_i^{new} = \alpha w_i^{old} + (1 - \alpha) w_i^{drain} \tag{6}$$

where $\alpha$ is a relaxation parameter ($0 < \alpha < 1$) which represents the flow resistance, and it is modeled as a cell attribute. In Equation (6), the value of $\alpha$ corresponds to the centre cell of the partition. In principle, a different $\alpha$ value can be assigned to every cell. Furthermore, for the purpose of modelling especial situations, the $\alpha$-field can be treated as a function of the water level. The latter will be a powerful tool in simulating water streamings.

*Surface-flow rule*

The surface flow is simulated by applying the water distribution rule acting sequentially on nine partitions of the spatial domain, in such a way that every cell occupies all the possible locations in the $3 \times 3$ basic partition. Figure 3 shows the partition sequence. It can be seen that the black cell is located in each of the nine positions of a $3 \times 3$ partition.

The time step acts once the distribution rule is applied to the complete sequence of nine partitions. The set of intermediate distributions is not considered 'observable', and should not be viewed as intermediate times, but only as auxiliary calculations, similarly to the sub-steps in the Runge-Kutta method (Butcher, 2003).

*Water sources*

Water additions to or subtractions from the cells, due to the precipitation and infiltration processes, are modeled as sources/sinks. Precipitations are simply added to each cell according to a predetermined time schedule, which can represent either actual measurements or hypothetical scenarios.

The infiltration process is more complicated than the precipitation, for its rate depends on the saturation state of the soil, which in turn changes when water infiltrates. In order to simulate this effect, it is necessary to keep track of the inventory, $I$ $(x, y)$, of water infiltrated in



DOI: 10.1002/hyp

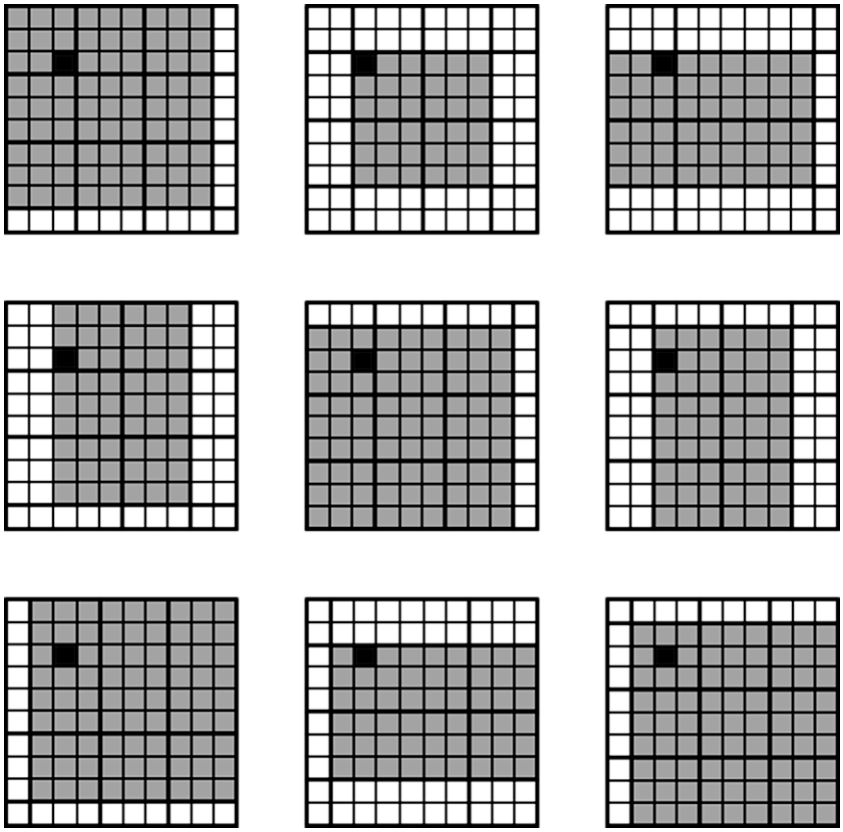

Figure 3. Sequence of partitions covering a step

each cell. The current infiltration volume at time step n is calculated as:

$$I_n(x, y) = \begin{cases} 0 \text{ if } w(x, y) = 0 \\ w(x, y) \text{ if } 0 < w(x, y) \\ \quad < \beta I_{n-1}(x, y) + I_o(x, y) \\ \beta\, I_{n-1}(x, y) + I_o(x, y) \text{ if } w(x, y) \\ \quad \geq \beta\, I_{n-1}(x, y) + I_o(x, y) \end{cases} \tag{7}$$

where $I_o(x, y)$ is a bias infiltration, and $\beta$ is a coefficient representing soil saturation characteristics ($0 < \beta < 1$). Smaller $\beta$ values mean that the soil would approach saturation faster. The initial infiltration, $I_1$, should be provided by the analyst, and it is likely to expect a dependence on the initial soil conditions.

*Creeks and rivers modelling*

Streams and rivers can be simulated in the AQUA environment by reducing the flow resistance along the corresponding water channels. Accordingly, the current value of $\alpha$ in every cell located along a river path is calculated as a function of the local water level, which accounts for the influence of the shape of the river bed on the flow rate.

Since there are a number of factors affecting this relation (bed profile, soil characteristics, aquatic vegetation, curvature, etc.) a comprehensive model would require the definition of a function for each cell. However, this is practically impossible when modelling large extensions of terrain. Alternatively, one can define regional families of $\alpha$-functions, whose parameters can be determined by comparing the numerical calculation with experimental data.

A function family that shows good agreement with flow measurements in southern streams of the Argentine Humid Pampas is the following:

$$\alpha_{river} = 1 - \alpha_o \left(\frac{w}{w_o}\right)^n \tag{8}$$

where $\alpha_o$, $w_o$ and $n$ are effective constant parameters.

*Boundary conditions*

Open boundary conditions are applied to the external contour of the simulated region. This is implemented by adding an auxiliary border consisting of two lines of cells with elevations substantially lower than the adjacent terrain (Figure 4). The water volume contained in the added border is eliminated after each calculation step, in order to avoid long-term accumulations. Inflows and outflows at any point of the terrain can be introduced as sources or sinks.

## APPLICATION OF THE MODEL TO REAL CASES

The AQUA model was applied to a plain region located at the centre of Buenos Aires Province, Argentina, between latitude south 36° 8′ and 37° 22′, and between longitude west 58° 49′ and 60° 10′. Its extension is about 150 km in Southwest–Northeast direction, and 40 km. wide, consisting of a large plain and a low hilly area at the



DOI: 10.1002/hyp

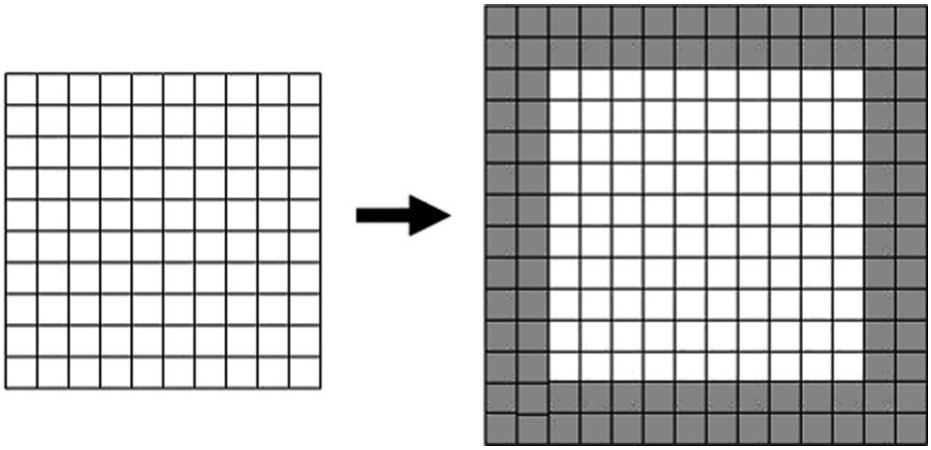

Figure 4. Treatment of the boundary conditions

southern boundary, where the Azul River headwaters occur. The hilly area is physiographically connected to the plains by pediments. Typical slopes are 5% in the south and less than 0·2% in the plain landscape (Sala *et al*., 1987).

Figure 5 shows the DEM constructed for this region. Given the extreme flatness of the terrain, the surface flow is very sensitive to minor topographic variations, and it is important that the DEM appropriately capture those variations. Unfortunately, the conventional technique of interpolation between the cartographic contour lines is inadequate, for all the details are lost in the process. In the present case, the model was produced by means of radar interferometry constructed from satellite images corresponding to the European Remote Sensing Satellite (ERS) Tandem mission in 1997. Synthetic Aperture Radar (SAR) interferometry is based on the relation between the phase difference of two radar scenes covering the study area and the corresponding terrain elevation. In theory, if the images are appropriately acquired, models with very good vertical resolutions can be obtained. However, it should be mentioned that there are several issues that should be carefully treated during the image processing, in order to correct typical distortions and reduce noise levels, which often appears in practical applications. Classical interferometric processing includes focusing, co-registration, interferogram generation and filtering, phase unwrapping, DEM generation and geocoding. The processing details involved in the DEM construction are described in (Euillades and Venere, 2003). The cell size of the resulting model shown in Figure 5 is 80 m. A number of small depressions can be observed in the lower region, which will be responsible for water stagnations. The vertical accuracy of the DEM is 1 m.

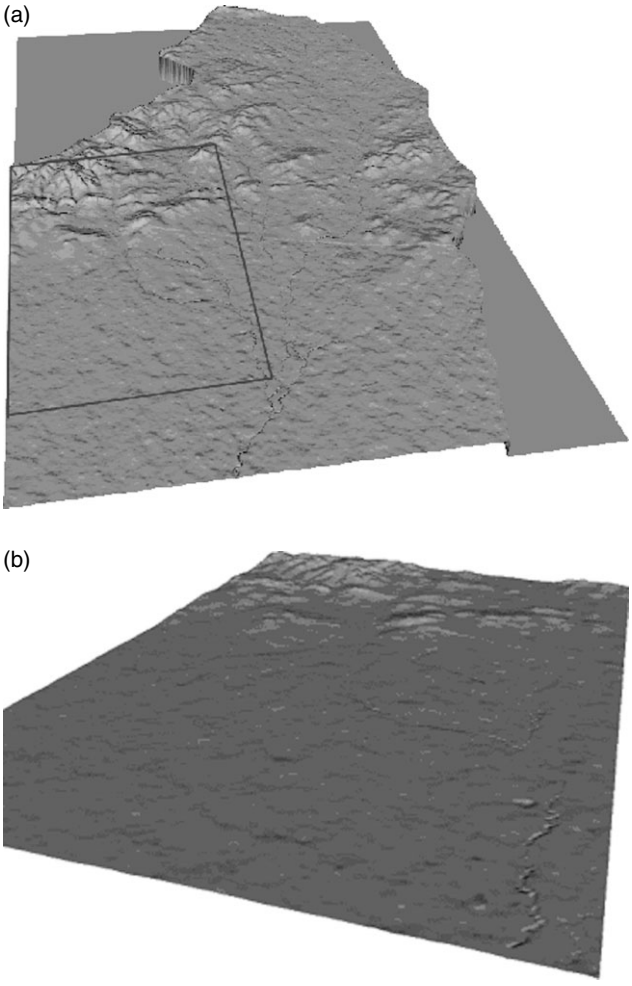


Figure 5. (a) Digital elevation model of the Azul basin. (b) Digital elevation model of the Santa Catalina sub-basin

The Azul basin, as well as the Pampas area, is sparsely populated. Most of the inhabitants live in urban areas. The ranches that occupy the land between towns are in the range of 100–5000 hectares. The land is mainly used for livestock and agriculture. The level of production is very high. The flooding is mainly caused by the heavy rainfall and, of lesser importance, by large discharge volumes from upstream areas. On average, the rainfall is 900 mm year$^{-1}$. However, in the last 30 years, the rainfall has increased up to 1200 mm year$^{-1}$. The most intense daily peaks (100–150 mm day$^{-1}$) happen in autumn and spring. Most of the excess water in the area disappears in the dry periods due to very intense evapotranspiration.

During the heavy rains, the rainfall does not infiltrate into the soil because it is waterlogged. The surplus



DOI: 10.1002/hyp

of water will therefore cause flooding, starting in the several small depressions. It has been a traditional practice, when flooding in the higher areas occurs, to dig small canals toward the lower sectors, to transfer the water downstream, generating disputes with owners of neighbouring lands. There are no natural collectors to drain such surpluses. Because of the low gradient, the water remains on the land for a long time, and the significant hydraulics processes are vertical instead of horizontal.

The region modeled in this study is the basin of the Santa Catalina Creek, which is a tributary of the Azul River. The length of the creek is 32 km, and drains 158 km$^2$ of the upper and middle sectors of the Azul River basin. Typical slopes in the upper basin are around 1–10% (rocky outcrops), whereas values of 0·1–1% characterize the middle sector. Most of the surface runoff is generated and channelled in the upper basin. The middle basin contributes little to the surface runoff, and basically receives the surplus generated in the upper basin. The Santa Catalina sub-basin contains numberless small depressions of the type above described, characteristics of large plains. As insignificant as it may seem given the mean discharge, the Santa Catalina Creek has contributed to relevant flooding of the Azul City, besides producing waterlogging of the rural areas it runs through.

The model was validated against major flood events that took place in May, August and October of 2002. The following hydrological data is available for each event:

- Integrated precipitation from pluviometers distributed along the basin.
- Temporal evolution of the rains measured in two points located at the upper part and at the lower part of the main river basin.
- Hydrograms of the Santa Catalina Creek, calculated from the HQ curve using water high data measured at the creek exit.
- (Phreatic) aquifer level previous to the rains.

Figure 6 compares the accumulated precipitation of the three events. The autumn event (May) is the largest in magnitude, presenting a pattern of a sequence of heavy rains. In turn, the events of winter (August) and spring (October) are shorter.

*Calibration of the model parameters*

In order to determine the timescale of the water flow process (i.e. the actual duration of every time step), it is necessary to compare the numerical outcomes with experimental measurements from real events. In the present case, the data corresponds to the flow response on the creek after a heavy rain during a short period of time (e.g. pulse precipitation), which typically produce a downstream flow wave. The effective model parameters were calibrated in the same way in order to minimize the differences between the numerical simulations and the actual data.

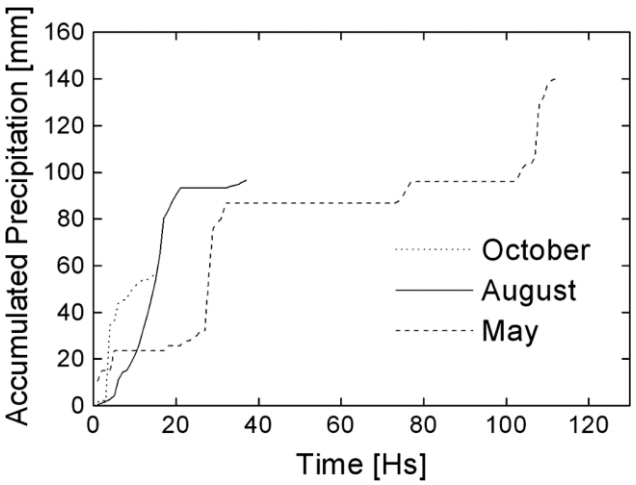


Figure 6. Accumulated precipitations in each event

The calibration is performed in two stages: general configuration and specific calibration. The purpose of the general configuration is to determine the time step corresponding to a single iteration. It is convenient to simulate the flow response on a river after a heavy rain during a short period of time (e.g. pulse precipitation), which typically produce a downstream flow wave. Several simulations of the transient are performed, increasing the value of $\alpha$ in the terrain and the river until the upper limit to ensure unconditional stability is determined. The time step is calculated equalling the arrival time of the downstream wave with the corresponding iteration number. Once the timescale is determined, simulations varying the infiltration parameters should be performed until the quadratic differences between the numerical simulations and the actual data are minimized.

Figures 7 and 9 show the hyetographs of precipitations in bars corresponding to the averaged water millimeters per hour. The solid points in the graphics represent the water flow discharged by the creek to the main river. Table I shows the resulting values of the effective parameters. The corresponding time step of each iteration is 3·6 s. It is important to note that, with the exception of

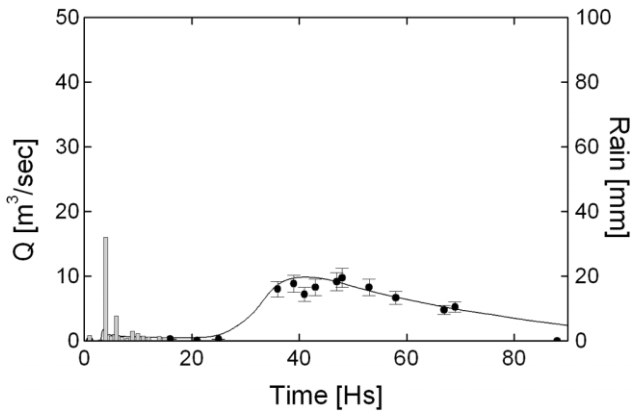


Figure 7. Measured (dots) and simulated (curve) outlet flow rate of the Santa Catalina Creek during the event of October 2002. The bars indicate the measured precipitation rate ($I_i = 10$, $I_o = 0{\cdot}5$, $\beta = 0{\cdot}9999$, $\alpha_{\text{terrain}} = 0{\cdot}99$, $\alpha_o = 0{\cdot}012$, $n = 3$)



DOI: 10.1002/hyp

Table I. Parameters used in the simulations of the real cases

| Parameter | May 2002 | August 2002 | October 2002 |
|---|---|---|---|
| $\alpha_{terrain}$ | 0·988 | 0·987 | 0·990 |
| $A_0$ | 0·012 | 0·012 | 0·012 |
| $n$ | 3 | 3 | 3 |
| $I_o$ (mm h$^{-1}$) | 0·5 | 0·5 | 0·5 |
| $I_i$ (mm h$^{-1}$) | 11 | 6 | 10 |
| $\beta$ | 0·9999 | 0·9999 | 0·9999 |

the terrain flow resistance ($\alpha$) and the initial infiltration ($I_1$), all the parameters are event-independent, which is an indication of the model robustness.

The October event was a typical spring rain, relatively mild and short. Figure 7 shows the hourly precipitation (bars) occurring during the first 20 h of the event. The points show the hydrograph of the downstream flow wave. The curve represents the numerical simulation of the flow wave response to the precipitation input.

The August case is a typical winter event, with continuous precipitations during a certain period of time. Figure 8 shows the hourly precipitation (bars) during the first 25 hof the event, with a mild recurrence between 30 and 40 h. The points and the curve show the measured downstream flow wave and the corresponding numerical simulation.

The May event is very interesting, for there were actually two consecutive rains separated by 80 h. The first rain acted by changing the humidity conditions for the second rain, saturating the absorption capacity of the soil. It can be seen in Figure 9 that the infiltration algorithm presented here is able to handle the whole event reproducing both waves with excellent agreement. It is worthwhile to note that these types of events are very difficult to simulate with models that use hyetographs based in curve numbers accounting for infiltrations and vegetation cover, e.g. the Hydrologic Modeling System from the Hydrologic Engineering Center (HEC-HMS).

The computational performance showed by the algorithm is very good. To simulate 1 h flow transient along

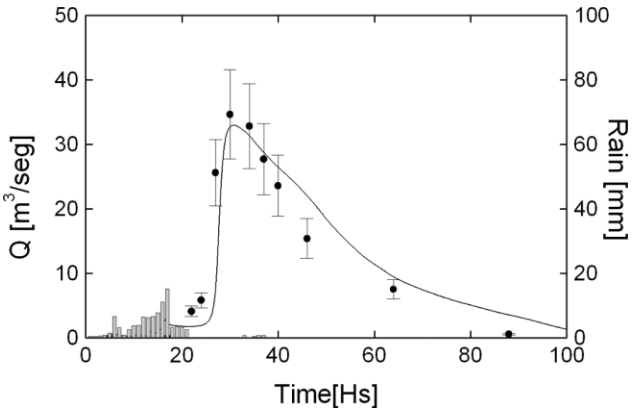


Figure 8. Measured (dots) and simulated (curve) outlet flow rate of the Santa Catalina Creek during the event of August 2002. The bars indicate the measured precipitation rate. ($I_i = 6$, $I_o = 0{\cdot}5$, $\beta = 0{\cdot}9999$, $\alpha_{terrain} = 0{\cdot}987$, $\alpha_o = 0{\cdot}012$, $n = 3$)

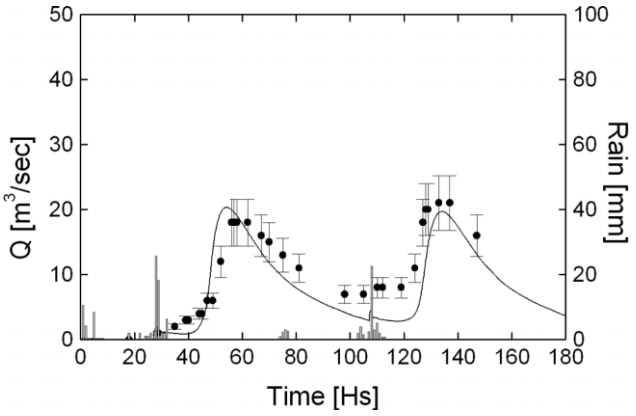


Figure 9. Measured (dots) and simulated (curve) outlet flow rate of the Santa Catalina Creek during the event of May 2002. The bars indicate the measured precipitation rate ($I_i = 11$, $I_o = 0{\cdot}5$, $\beta = 0{\cdot}9999$, $\alpha_{\text{terrain}} = 0{\cdot}988$, $\alpha_o = 0{\cdot}012$, $n = 3$)

6400 m$^2$ (192 × 299 cells), the calculation takes 27 s in a Pentium IV 3 GHz 1 GB RAM.

It can be seen that the simulation reproduces the measurements fairly well. The calibration could be achieved with uniform parameter values over the whole creek basin. Season dependence was found in the initial infiltration and in the surface-flow resistance parameter, which is reasonable since both are influenced by the current soil conditions. Indeed, the initial infiltration capacity of the soil depends on the soil water content, and the flow resistance is strongly influenced by the vegetation, which varies substantially along the year.

It is interesting to note that although the present model does not include a surface storage coefficient in the cells (as most models do), the measurements are reproduced fairly accurately. The reason for this performance is that the calculation is based on a digital topological representation defined over a very fine mesh, which captures the terrain depressions responsible for the surface water storage. Figure 10 compares the map of waterloggings calculated with the present model with an average of satellite observations (i.e. the flooding potential risk map), showing very similar patterns.

## SENSITIVITY ANALYSIS

In order to determine the robustness of the model, the sensitivity of the simulation results to variations of the relevant parameters was studied. The parameters analysed were the terrain and river relaxation factors and the infiltration coefficients. Each parameter was varied about a reference value, keeping constant all the other parameters. The Santa Catalina event of May 2002 was used as reference (Table I), since the two sequential flooding waves that were registered during that event are useful to observe the sensitivity at different timescales.

The parameter $\alpha_{terrain}$ is defined in Equation (6), and represents the flow resistance due to vegetation and soil friction. The sensitivity of the results to $\alpha_{terrain}$ variations is shown in Figure 11. It can be seen that as $\alpha_{terrain}$



DOI: 10.1002/hyp

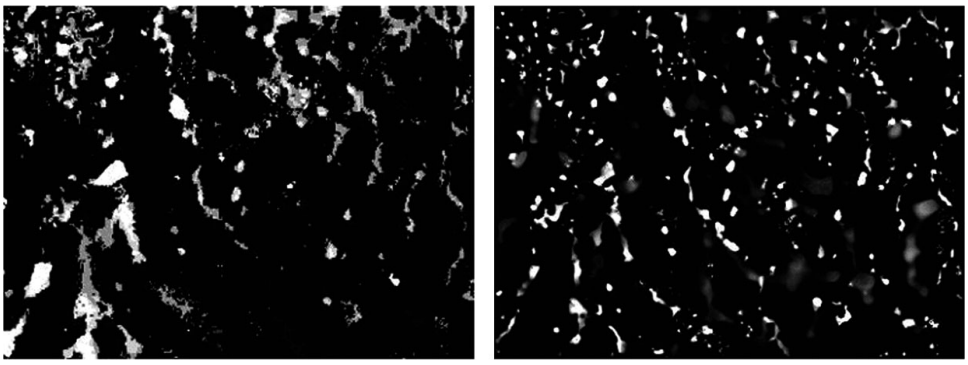

Figure 10. Observed (left) and calculated (right) flooding patterns

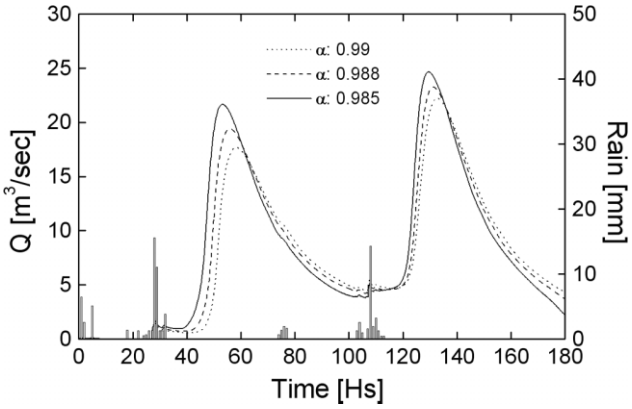


Figure 11. Sensitivity to the parameter $\alpha$ of the terrain

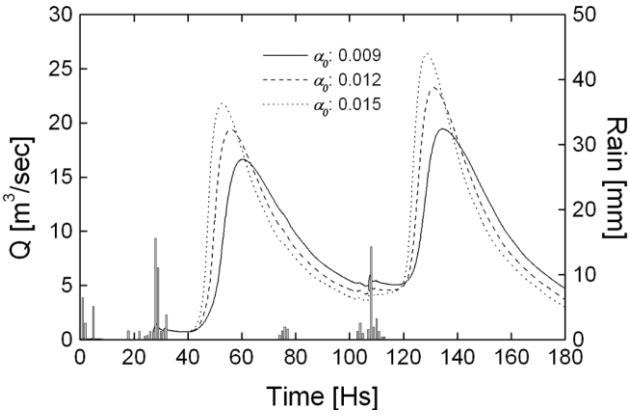


Figure 12. Sensivility to the infiltration coefficient $\alpha_o$

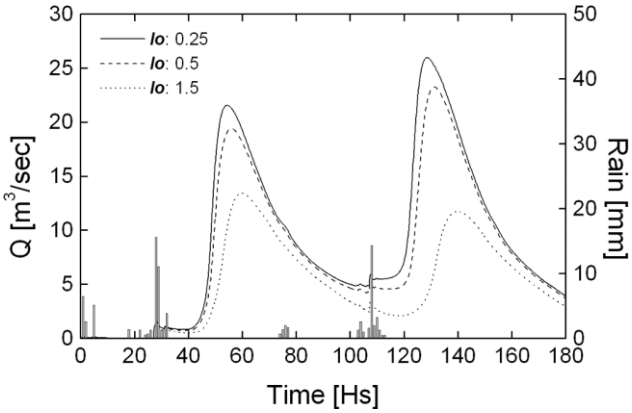


Figure 13. Sensivility to the infiltration bias $I_o$

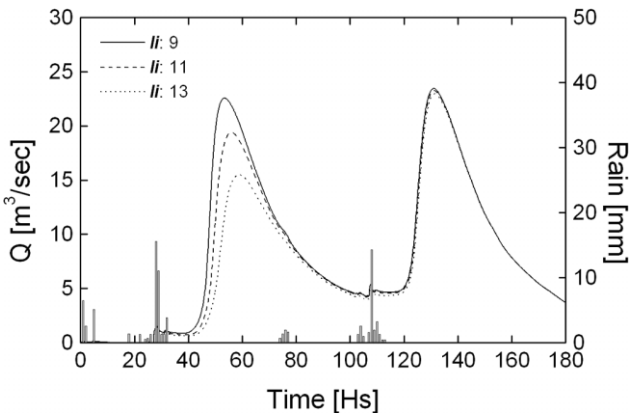


Figure 14. Sensivility to the initial infiltration $I_i$

decreases the flooding peaks are higher and occur faster. The latter is due to the fact that the water moves faster, which in turn reduces the infiltration causing higher flow rates.

The coefficient $\alpha_o$ is defined in Equation (8), and plays in the river, the opposite role of $\alpha_{terrain}$, that is, the flow resistance of the river increases as $\alpha_o$ decreases. Figure 12 shows the sensitivity of the simulation results to variations of $\alpha_o$. It can be seen that larger values of $\alpha_o$ produce higher flow rates in the river and narrower peaks. The latter is due to the fact that the river flow rate accelerates as the water level increases, and this effect is enhanced at larger $\alpha_o$.

The infiltration Equation (7) can be seen as an exponential decay from an initial value $I_1$ to a saturation bias $I_o$, $\beta$ being the saturation rate coefficient. Figure 13 shows the sensitivity of the results to variations of $I_o$. It can be seen that since $I_o$ governs the average absorption capacity of the terrain, larger values of this parameter reduce the surface flow. Figure 14 shows the impact of the infiltration capacity of the soil at the beginning of the event, $I_1$. It can be seen that changes in $I_1$ only affect the flow rate during the first part of the event ($t < 80$ h), after which the soil reaches its infiltration capacity. Figure 15 shows the sensitivity of the simulation to variations of the saturation coefficient $\beta$. Larger



DOI: 10.1002/hyp

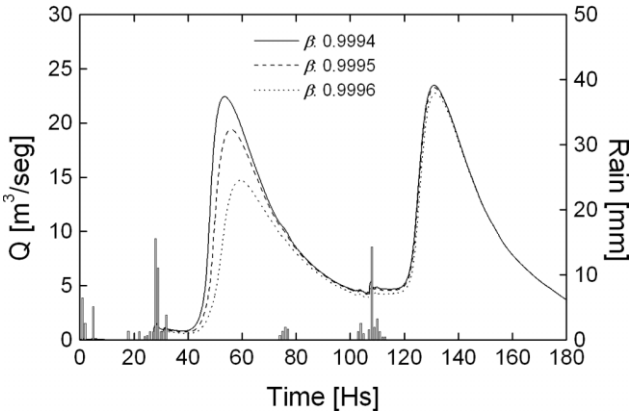


Figure 15. Sensibility to the saturation coefficient $\beta$

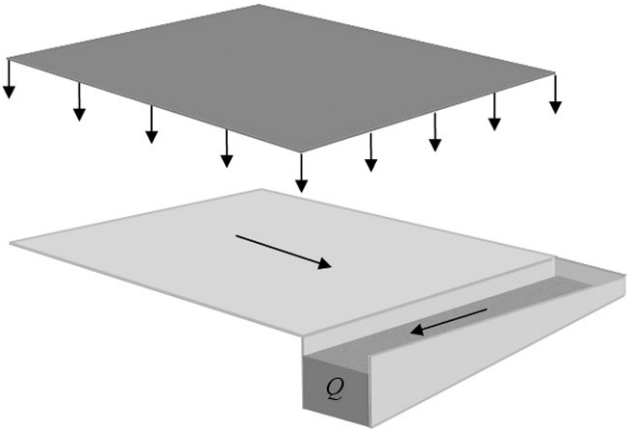


Figure 16. Ideal surface-flow case

values of $\beta$ induce faster saturation of the soil, and consequently, the impact of the infiltration is larger in magnitude and duration.

## COMPARISON AGAINST OTHER SURFACE-FLOW MODELS

In order to test the coherence of the theory, the present model was also compared against HEC-1, a well- known surface water flow simulator. The test was performed in the synthetic scenario shown in Figure 16, representing a simple plain with an adjacent channel. The size of the plain is 8800 by 11 000 m with a slope 0·0085. The water drains to a rectangular channel 5 m wide with a slope of 0·0025.

Table II. Parameters used in the simulations of the synthetic case

| | |
|---|---|
| $\alpha_{terrain}$ | 0·988 |
| $\alpha_o$ | 0·012 |
| $n$ | 3 |
| $I_o$ (mm hora$^{-1}$) | 0 |
| $I_1$ (mm hora$^{-1}$) | 0 |
| $\beta(x, y)$ | 0·9999 |

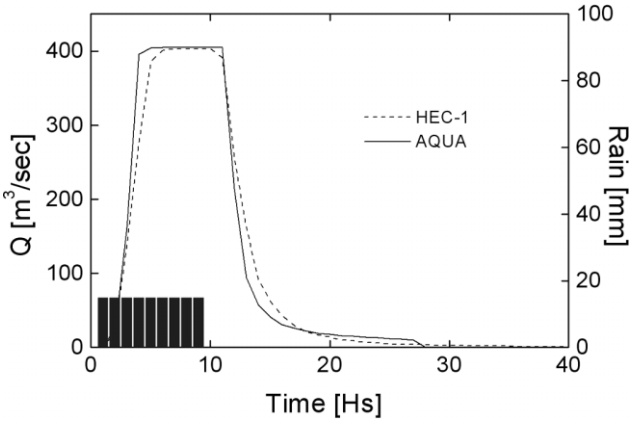


Figure 18. Channel flow in after a constant rate of 15 mm h$^{-1}$ during 10 h in the plain

The parameters used in the simulation are shown in Table II. The equivalent *Manning* coefficients used by HEC-1 in the plain and the channel are 0·02 y 0·01 respectively, corresponding to the minimum roughness. Figures 17 and 18 show the channel outlet flow for two different events, both corresponding to a uniform rain over the plain. It can be seen that the present model matches the standard results pretty fairly.

## CONCLUSIONS

Surface water modelling in large plains deserves special attention owing to the different mechanisms that may

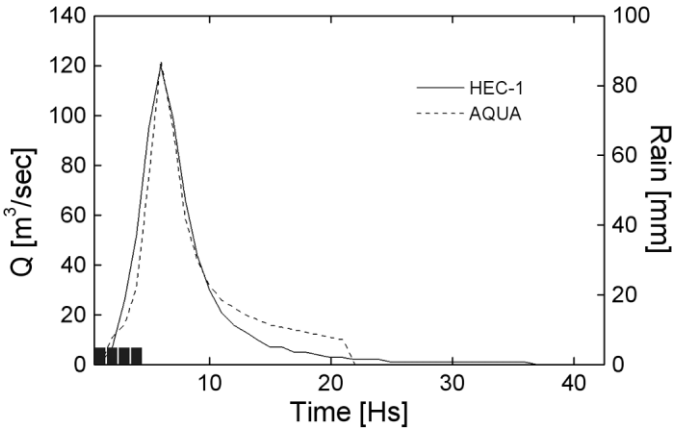


Figure 17. Channel flow in after a constant rate of 5 mm h$^{-1}$ during 5 h in the plain (Figure 18)



DOI: 10.1002/hyp

lead to flooding as opposed to what may be expected in sloping terrains. Given the paramount importance of small differences in the topographical relief, the heterogeneity and drainage characteristics of soils, the influence of depressions that accumulate rainwater, and the low energy available to produce channelled surface flow, most of the conventional models fail in representing adequately the observed flooding patterns.

A novel approach was presented in this article, which falls into the distributed hydrological model category. It has been proven that, for the model to function properly, the domain (no matter how large) has to be partitioned in small cells that reflect the short scale topology. The type and current local moisture of the soil is characterized in each cell by a relaxation parameter ($\alpha$) that determines how fast the water will move onto the land or in the watercourses, and an infiltration function ($I$) to address the water entering the vadose zone. The surface water excess is distributed according to the elevation differences between adjacent cells, for which it has been demonstrated that counting on a fine-quality DEM is an unavoidable pre-condition.

Even though the AQUA algorithm follows a CA rationale, and so it is not a physically based model, the results of the algorithm closely resemble the behaviour of natural flows. It can be seen in Figure 12 that as the parameter $\alpha$ increases, the flow velocity also increases, which suggests an inverse relation to Manning's $n$ and a direct relation to Strickler's roughness coefficient. The power law in Equation 8 is a quite common form for surface-flow equations; in fact, Manning's equation stems from an equation that is a kind of a power law. The variation in computed channel flow velocities is qualitatively analogue to what would be expected from Saint Venant equations. Notwithstanding those encouraging results, the relation between the Aqua algorithm and the fluid mechanics laws governing the simulated phenomena should be the object of further research.

The model at hand (AQUA) has been able to reproduce the measured channelled flow from single and multi-pulse rainfall events at a basin located in the centre of Buenos Aires Province, as well as to match pretty closely the regional flooding pattern from satellite imagery. Additionally, AQUA was compared to a model known worldwide (HEC-1) revealing an excellent agreement. While it has been shown (Hunter *et al*., 2005) that small variations in free surface can be approximated by a diffusion system, there are problems with computation times and stability. The linear approach of the present model bypasses this problem, and therefore the system showed unconditional stability in all the cases studied.

Because of the large time span of water ponded on the surface in large plains, a future improvement will have to incorporate a sink parameter to account for the water lost through evapotranspiration.

## ACKNOWLEDGEMENTS

This project was supported by the National Agency for Science, Technology and Innovation of Argentina (PID 165), the Scientific Research Council of the Buenos Aires Province (CICPBA), and the National Atomic Energy Commission from Argentina (CNEA). The satellite images were provided by the National Space Agency of Argentina (CONAE).

## REFERENCES

Abbott MB, Bathurst JC, Cunge JA, O'Conell PE, Rasmussen J. 1986. An introduction to the European hydrological system–Systeme Hydrologique Européen "SHE": 2. Structure of a physically-based, distributed modeling system. *Journal of Hydrology* **87**: 61–77.

Butcher J. 2003. *Numerical Methods for Ordinary Differential Equations*, 2nd edn. John Wiley and Sons: Chichester, UK.

Cooper NG (ed.). 1987. *Los Alamos Science Special Issue*. Los Alamos National Laboratory: New Mexico.

Euillades P, Vénere M. 2003. Corrección de modelos de elevación en base a un conjunto de puntos seguros. *Revista Internacional de Métodos Numéricos Para Cálculo y Diseño en Ingenieria* **19**: 33–43.

Freeze RA, Harlan RL. 1969. Blueprint for a physically-based, digitally-simulated hydrologic response model. *Journal of Hydrology* **9**: 237–258.

Hunter NM, Horritt MS, Bates PD, Wilson MD, Werner MGF. 2005. An unconditionally stable explicit solution for raster-based storage cell modelling of floodplain inundation. *Advances in Water Resources* **28**: 975–991.

Sala JM, Kruse E, Aguglino R. 1987. *Investigación hidrológica de la Cuenca del Arroyo Azul, Provincia de Buenos Aires*. CIC, Informe 37.

Varni M, Usunoff E, Weinzettel P, Rivas R. 1999. Groundwater recharge in the Azul aquifer, central Buenos Aires province, Argentina. *Physics and Chemistry of the Earth* **24**: 349–352.

Wolfram S. 1986. Cellular automata fluids. *Journal of Statistical Physics* **45**: 3–4.




DOI: 10.1002/hyp